Appl. Phys. B 91, 295–298 (2008)
DOI: 10.1007/s00340-008-2979-5

Applied Physics B
Lasers and Optics

L. JI[1]
P. LU[1,✉]
N. DAI[1]
J. ZHANG[1]
Z. YANG[1]
Y. LI[1]
W. CHEN[2]
Z. JIANG[2]
J. LI[2]

Multiplex frequency conversion of femtosecond laser pulses in trefoil and quatrefoil channels of a holey fiber

[1] Wuhan National Laboratory for Optoelectronics, Huazhong University of Science and Technology, Wuhan 430074, P.R. China
[2] Fiberhome Telecommunication Technologies Co. Ltd., Wuhan 430074, P.R. China

Received: 29 August 2007/Revised version: 19 January 2008
Published online: 27 March 2008 • © Springer-Verlag 2008

ABSTRACT We report that trefoil and quatrefoil silica channels with sizes ranging from 0.6 μm to as large as 4–5 μm in a holey fiber can strongly confine the light field and act as highly nonlinear waveguides. Supercontinuum emissions, efficient dispersive-wave generation and parametric four-wave-mixing processes were achieved in these channels with sub-nanojoule femtosecond Ti:sapphire laser pulses. Two dispersion curves corresponding to two orthogonal modes in each channel were simulated and used to explain the experimental results.

PACS 42.81.Gs; 42.81.Qb

1 Introduction

Photonic crystal fibers (PCFs) have been a subject of intense research activity for the past few years. Nonlinear optics of ultra-short laser pulses in PCFs is one of the most interesting and rapidly growing areas. PCFs can largely enhance nonlinear interactions of laser pulses because of the strong confinement of the light field in the fiber core [1] and tailored dispersion characteristics of guided modes [2]. Nonlinear optical processes such as supercontinuum generation [3–6] and nonlinear frequency conversion [7–11] have been achieved with PCFs. Tunable supercontinuum emissions were achieved in a single PCF that has multiple sub-micron cores [12]. Parametric four-wave-mixing (FWM) processes in sub-micrometer-scale secondary cores of holey fibers were reported recently [13]. Secondary cores in holey fibers [7, 13, 14] or sub-micron cores in multi-core microstructure fibers [5, 12] can strongly confine the light field, leading to a substantial waveguide enhancement of nonlinear optical processes. Theoretical studies have demonstrated that the waveguide enhancement of nonlinear optical processes reaches its maximum at a certain optimal value of the fiber-core size, corresponding to the maximum ratio of the laser power confined in the fiber core to the diameter of the fiber core [5]. The optimal waveguide channel diameter for nonlinear optical processes with high efficiency in holey fibers has been demonstrated to lie in the sub-wavelength range. Enhanced nonlinear optics of micron waveguides in PCFs has potential application in multiplex frequency converters and supercontinuum generators.

In this paper, we demonstrate that trefoil and quatrefoil channels present between the holes of a microstructure fiber having a large air-filling fraction (87%) can serve as highly nonlinear waveguides. Supercontinuum emission, parametric four-wave-mixing processes and efficient dispersive-wave generation were achieved in the fiber. Sizes of the channels used in this paper range from 0.6 μm to as large as 4–5 μm. The maximal size of the channels is larger than those used in earlier reported works [5, 7, 12–14]. To our knowledge, there is no report about frequency conversion of sub-nanojoule femtosecond Ti:sapphire laser pulses in such large channels as efficient as in this work. The physical scenarios of the nonlinear optical spectral transformations are explained in virtue of the calculated dispersion curves.

2 Holey fiber and experimental setup

The holey fiber used in this study was fabricated with fused silica using the standard stack-and-draw technique. A scanning electron microscopy (SEM) image of the cross-sectional structure of it is shown in Fig. 1. The fiber contains five rings of air holes surrounding a large air hole with a diameter of 23.0 μm; the air-filling fraction is about 87%. We choose three typical channels to carry out the experiment. One is a trefoil channel surrounded by three air holes. The dimension of it is about 0.6 μm. The other two are quatrefoil channels surrounded by four air holes; the width and length of them are about 2–3 μm and 4–5 μm.

Experiments were performed with a Ti:sapphire laser (Tsunami, Spectra-Physics) running at a central wavelength of 796 nm with a pulse-repetition rate of 82 MHz. The maximum average output power of the laser is 400 mW. The duration of laser pulses launched into the fiber was about 50 fs. The fiber was placed on a three-dimensional (XYZ) translation stage. The input beam launched into channels 1–3 as marked in Fig. 1 was focused by a micro-objective (NA = 0.65). A CCD camera was used for imaging and ascertaining the spot of the laser beam launched into the channels.

✉ Fax: +86-27-87543755, E-mail: lupeixiang@mail.hust.edu.cn

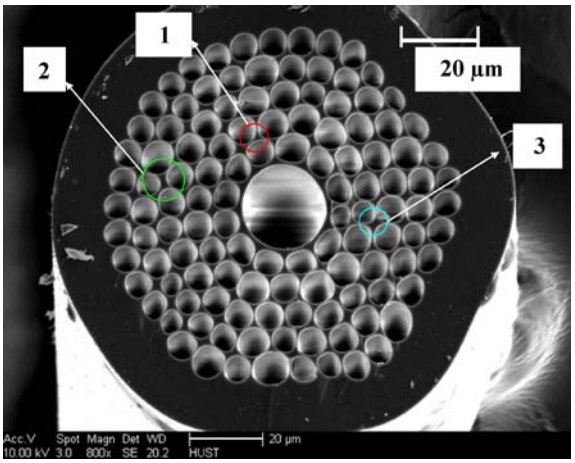

FIGURE 1 Scanning electron micrograph of the holey fiber; three channels are shown with *white panes*

A near-field end-face image of light transmitted in the fiber was obtained by a micro-objective (NA = 0.65) and another CCD camera. Spectral measurements were performed by an optical spectrum analyzer (Ocean Optics) with a wavelength range of 400–1100 nm.

3 Experimental results and discussion

In this experiment, laser pulses were carefully launched into the three channels of the fiber with a length of 2.0 m. Output emissions generated in channels 1–3 differ both visually and in their significant spectral properties. Figure 2a–c present far-field beam profiles of the blue-shifted emissions at 2.0-cm distance from the fiber end; the output average power from channels 1–3 was 60 mW. Figure 2d–f show the side images of the fiber. The fiber displayed orange, green and blue colors by launching laser pulses into channels 1–3, respectively. Near-field images of the fiber output ends for laser pulses launched into a trefoil channel (corresponding to channel 1) and a quatrefoil channel (corresponding to channel 3) are shown in Fig. 2g–h. They demonstrate that the laser pulses were strongly confined in the individual channels. From the near-field image (Fig. 2g) for channel 1, there is no significant coupling between adjacent 'cores'. However, for channel 3 (Fig. 2h), there is a slight coupling between adjacent cores. From the above, the losses in the channels are not equal. In the discussion of the experiments, we neglected the losses

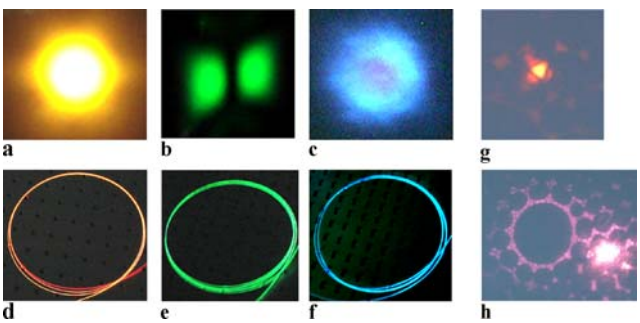

FIGURE 2 Far-field images of output emission (**a–c**), side images of the fiber (**d–f**) and near-field images of the fiber output (**g** and **h**)

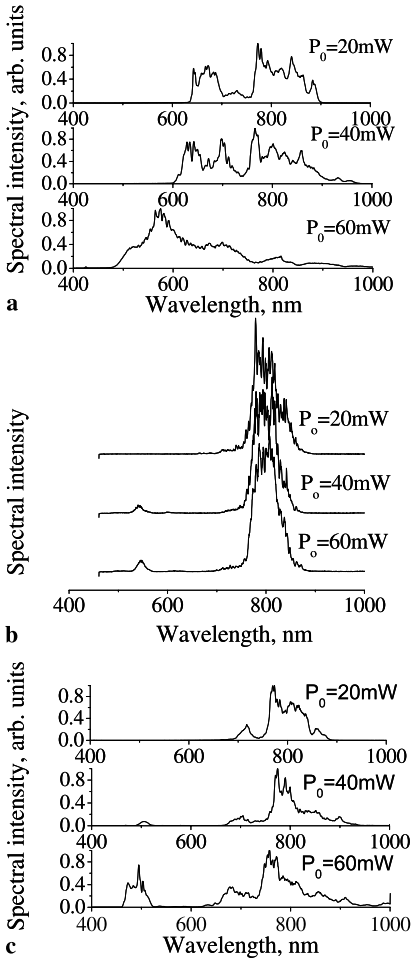

FIGURE 3 Spectra of output beam from channels 1–3 (**a–c**). The pump power launched into each channel is labeled in each graph

in the channels. The average powers labeled in Fig. 3 are output powers from the fiber. Typical optical spectra measured directly from the output of the fiber are presented in Fig. 3.

We set up models based on SEM of the fiber-channel structures to simulate the light propagation in these channels with the finite-element method. A portion of the fiber comprising one or two silica cores with air holes was modeled with anisotropic perfectly-matched-layer (PML) boundary conditions. Light propagates through channel 1 in the fundamental mode (FM) as shown in Fig. 2a and g. The blue-shifted emission in channel 2 (Fig. 2b) has a beam shape corresponding to the second-order PCF spatial mode (Fig. 4, M3 and M4). There is red light in the center of the far-field image of the output emission from channel 3; we think that the blue-shifted light is in a FM mode. The secondary cores are surely birefringent for their strong form anisotropy. Simulation results for the mode-intensity distribution and polarization distribution of the FM, the second-order mode and the FM at 800 nm in channel 1, channel 2 and channel 3 are shown in Fig. 4. M1 and M2 are two orthogonal modes of the FM in channel 1. M3 and M4 are second-order modes in channel 2. M5 and M6 are corresponding to two orthogonal modes of the FM in channel 3. The group velocity dispersion (GVD) curves of the related mode propagation in channels 1–3 calculated by the finite-element method are shown in Fig. 5. However, in the

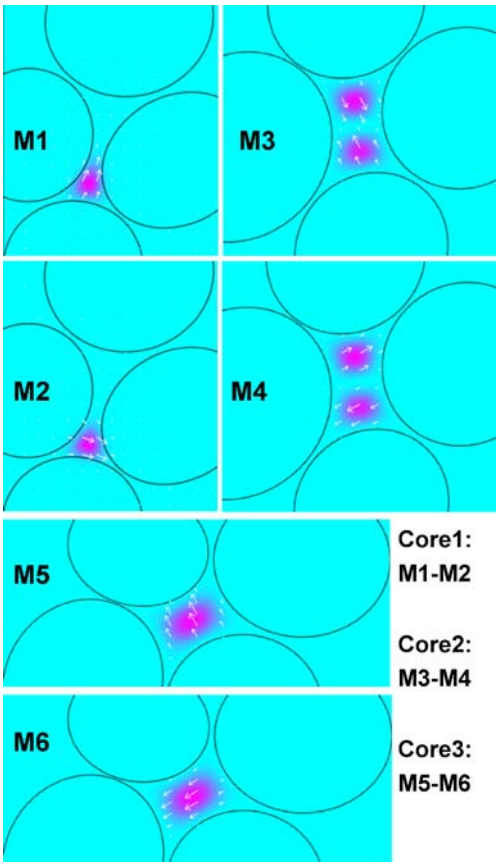

FIGURE 4 Simulation results for mode intensity distribution and polarization distribution of the FM, the second-order mode and the FM at 800 nm in channel 1 (M1, M2), channel 2 (M3, M4) and channel 3 (M5, M6)

experiment the birefringence effect was not considered adequately.

Supercontinuum emission was obtained in channel 1 (Fig. 3a). The blue-shifted emission became stronger and moved towards shorter wavelengths with increasing input power. With pump power increasing to 60 mW, the output spectrum extended from 480 to 1000 nm and was peaked around 570 nm. To explain the experimental results, the group-velocity dispersion of light propagation in the channel should be considered. As shown from Fig. 5, the spectrum of the input field is in the region of anomalous dispersion for the guided mode in channel 1. The laser pulses tend to form optical solitons as they propagate through the channel. Red-shifted radiation results from the phenomenon of soliton self-frequency shift. The central wavelength of the red-shifted soliton at the output beam is controlled by the input power and becomes longer with increase of input power. The blue-shifted radiation is formed due to interaction between solitons and dispersive waves seeded from the initial soliton fission [6, 15–17]. The presence of higher-order dispersion can lead to the transfer of energy from the soliton to a narrow-band resonance in the normal GVD regime. This is demonstrated in the bottom graph in Fig. 3a. The blue-shifted emissions are clearly stronger than the pump and the red-shifted part.

As shown in Fig. 3b, green light peaking at 540 nm came from channel 2 by launching laser pulses. In the experiment

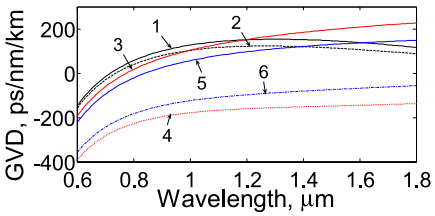

FIGURE 5 Group velocity dispersion profiles of the related modes (M1–M6, corresponding to Fig. 4) calculated for the three channels

the polarization orientation of the pump was not selected specifically; so, the pump was possibly in the anomalous dispersion regime for the second-order mode in channel 2, but no supercontinuum generation is obtained. The blue-shifted emission is considered to be the signal coming from a FWM process $2\omega_p = \omega_a + \omega_s$. The frequency component belongs to the spectrum of the input laser field. The process leads to the generation of signal and idler sidebands with central frequencies ω_a and ω_s. The phase-matching condition for this process should be written as $\delta\beta = \beta(\omega_a) + \beta(\omega_s) - 2\beta(\omega_p) + 2\gamma P_1 = 0$, where $\beta(\omega)$ is the propagation constant of the field spectral component with frequency in a given fiber mode, γ is the nonlinear parameter at the pump wavelength and P_1 is the peak power of pump light. The central wavelength of green light remained nearly constant with increasing pump power, since the nonlinear term $2\gamma P_1$ is too small to affect the phase-matching condition in experiments. The conversion efficiency of the FWM process is low for small nonlinear parameters or other reasons such as the polarization state of the pump beam not being optimal for the FWM process. The infrared idler light was not displayed in Fig. 3b since the wavelength range of the optical spectrum analyzer used is only 400–1100 nm.

Figure 3c shows the spectra of emissions emerging from channel 3. With 20-mW pump power launched into channel 3, a supercontinuum emission ranging from 700 to 880 nm was obtained. A blue-shifted sideband peaking at 504 nm appeared along with a supercontinuum emission ranging from 660 to 920 nm when the pump power was 40 mW. The blue-shifted sideband became stronger and shifted to shorter wavelengths with increase of pump power. With 60-mW laser pump, the blue-shifted emission centered at 495 nm took about 20% of all the intensity of the output beam. From Fig. 5, as the pump wavelength approaches the zero-dispersion wavelength (ZDW) but still lies within the normal GVD regime, the initial spectral broadening due to parametric four-wave mixing and self-phase modulation (SPM) transfers spectral content into the vicinity of the ZDW and across into the anomalous GVD regime [6, 17, 18]. The long-wavelength part of the spectrum falls within the region of anomalous dispersion and can form solitons. These solitons undergo a continuous frequency down-shift due to soliton self-frequency shift. The blue signal is likely to be dispersive waves or third-harmonic generation from a soliton self-frequency shifting into the 1.3–1.6 μm range. However, if the blue signal was the third harmonic of the solitons, it must be very weak. This is opposite to the experimental result, so we can exclude this reason. Higher-order dispersion induces wave-matching resonances between solitons and dispersive waves, leading to intense emissions, and they become an intense spectral band.

4 Conclusions

In this paper, quatrefoil silica channels with width of about 2–3 μm and length of about 4–5 μm in a holey fiber were demonstrated to be highly nonlinear waveguides with high birefringence. Multiplex frequency conversion of sub-nanojoule Ti:sapphire femtosecond laser pulses in the trefoil and quatrefoil channels was obtained. Due to parametric four-wave-mixing processes, green light peaking at 540 nm came from the channel where the pump wavelength was in the range of anomalous dispersion. An efficient dispersion wave near 470–510 nm in concomitance with a supercontinuum extending from 650 to 1000 nm was achieved in the channel where the pump wavelength was in the range of normal dispersion. In our work, it is unusual to achieve so efficient nonlinear optical spectral transformations in the large waveguide channels. In a silica channel with dimension of about 0.6 μm, the pump wavelength falls within the range of anomalous dispersion; a supercontinuum extending from 480 to 1000 nm was obtained. These nonlinear optical spectral transformations in each channel were explained reasonably in virtue of the calculated dispersion curves.

ACKNOWLEDGEMENTS This work was supported by the Specialized Research Fund for the Doctoral Program of Higher Education of China under Grant No. 20040487023 and the National Key Basic Research Special Foundation under Grant No. 2006CB806006.

REFERENCES

1 P.S.J. Russell, Science **299**, 358 (2003)
2 W.H. Reeves, D.V. Skryabin, F. Biancalana, J.C. Knight, P.S.J. Russell, F.G. Omenetto, A. Efimov, A.J. Taylor, Nature **424**, 511 (2003)
3 J.K. Ranka, R.S. Windeler, A.J. Stentz, Opt. Lett. **25**, 25 (2000)
4 J. Herrmann, U. Griebner, N. Zhavoronkov, A. Husakou, D. Nickel, J.C. Knight, W.J. Wadsworth, Phys. Rev. Lett. **88**, 173 901 (2002)
5 D.A. Akimov, M. Schmitt, R. Maksimenka, K.V. Dukel'skii, Y.N. Kondrat'ev, A.V. Khokhlov, V.S. Shevandin, W. Kiefer, A.M. Zheltikov, Appl. Phys. B **77**, 299 (2003)
6 J.M. Dudley, G. Genty, S. Coen, Rev. Mod. Phys. **78**, 1135 (2006)
7 J.H.V. Price, T.M. Monro, K. Furusawa, W. Belardi, J.C. Baggett, S. Coyle, C. Netti, J.J. Baumberg, R. Paschotta, D.J. Richardson, Appl. Phys. B **77**, 291 (2003)
8 S.O. Konorov, A.M. Zheltikov, Opt. Express **11**, 2440 (2003)
9 F.G. Omenetto, A. Taylor, M.D. Moores, J.C. Knight, P.S.J. Russell, J. Arriaga, Opt. Lett. **26**, 1558 (2001)
10 A. Efimov, A.J. Taylor, F.G. Omenetto, J.C. Knight, W.J. Wadsworth, P.S.J. Russell, Opt. Express **11**, 2567 (2003)
11 J.K. Ranka, R.S. Windeler, A.J. Stentz, Opt. Lett. **25**, 796 (2000)
12 M.L. Hu, C.Y. Wang, Y.F. Li, Z. Wang, L. Chai, Opt. Express **12**, 6129 (2004)
13 P. Dupriez, F. Poletti, P. Horak, M.N. Petrovich, Y. Jeong, J. Nilsson, D.J. Richardson, D.N. Payne, Opt. Express **15**, 3729 (2007)
14 A.B. Fedotov, S.O. Konorov, E.E. Serebryannikov, D.A. Sidorov-Biryukov, V.P. Mitrokhin, K.V. Duke'skii, A.V. Khokhlov, V.S. Shevandin, Y.N. Kondrat'ev, M. Scalora, A.M. Zheltikov, Opt. Commun. **255**, 218 (2005)
15 P.A. Wai, C.R. Menyuk, Y.C. Lee, H.H. Chen, Opt. Lett. **11**, 464 (1986)
16 P.A. Wai, H.H. Chen, Y.C. Lee, Phys. Rev. A **41**, 426 (1990)
17 N. Akhmediev, M. Karlsson, Phys. Rev. A **51**, 2602 (1995)
18 S. Coen, A.H.L. Chau, R. Leonhardt, J.D. Harvey, J.C. Knight, W.J. Wadsworth, P.S.J. Russell, J. Opt. Soc. Am. B **19**, 753 (2002)